# *A novel friction model for predicting nonlinear friction dynamics*

Article

Accepted Version

## www.reading.ac.uk/centaur

## CentAUR

Central Archive at the University of Reading

Reading's research outputs online

# A novel friction model for predicting non-linear friction dynamics

Authors: Anthony Nnaji,
e-mail: anthony.nnaji@esut.edu.ng
Electrical and Electronic Engineering Department, Enugu State University of Science and Technology, Enugu, Nigeria
William Holderbaum,
e-mail: w.holderbaum@reading.ac.uk
Department of Biomedical Engineering, University of Reading, Reading, United Kingdom
Victor Becerra,
e-mail: victor.becerra@port.ac.uk
School of Energy and Electronic Engineering, University of Portsmouth, Anglesea Building, Anglesea, Portsmouth, United Kingdom

**Abstract:** In this paper a new dynamic friction model capable of modeling observed friction dynamics is presented. The model incorporates a pre-sliding friction function with non-local memory hysteresis features. Simulations showed the model's ability to predict known friction features. An experimental test-bed was developed and used for friction characterization through a carefully designed set of experiments. The new model has one parameter more than the LuGre model, which are easy to estimate through system identification. System identification was performed to determine parameters of the proposed friction model as well as the LuGre and GMS models for the purposes of model performance comparison. Experimental and simulation results of the new dynamic friction model with the identified model parameters exhibited a strong correspondence with the results of the characterization experiments, capturing known friction features. The new friction model being simple both in structure and implementation demonstrated superior capability for modeling friction phenomena than the LuGre and GMS friction models.

**Index Terms:** Friction regimes, friction dynamics, friction models, characterization experiment, Stribeck effect, system identification.

**Biographical notes:** Anthony Nnaji received the B.Eng degree in Electrical and Electronics Engineering from the University of Benin, Edo State, Nigeria in 1999 and the M.Eng degree from Enugu State University of Science and Technology, Enugu state, Nigeria, in 2006. He also obtained his Ph.D degree in Control Systems Engineering from the School of Systems Engineering, University of Reading, Reading, U.K., in 2017. Dr. Nnaji is currently a lecturer with the Electrical and Electronics Engineering Department, Enugu State University of science and Technology, Enugu state, Nigeria. His research interests include systems modeling and control with particular interest to nonlinear system, energy storage systems control and power systems stability and control.

William Holderbaum received the PhD degree in electrical engineering from the University of Lille, Lille, France, in 1999. He was a research assistant with the University of Glasgow, Glasgow, U.K.., from 1999 to 2001. He joined the University of Reading, Reading, U.K., in 2001, as a Lecturer and then became a senior Lecturer/Associate Professor. Currently, he is a Professor of Mathematical engineering with the School of Systems Engineering. His research interests include control theory and its applications. These are mainly focused on geometric control theory, in particular, Hamiltonian systems and optimization problems. This research uses the mathematical engineering skills in order to model and control non-linear systems. His research interests also include control with application to rehabilitation engineering, energy reduction, smart grid, multiple agent systems, fuel cells, power generation, and autonomous vehicles.

Victor Becerra received the B.Eng degree in electrical engineering from Simon Bolivar University, Caracas, Venezuela, in 1990, and the Ph.D. degree in control engineering from City University, London, U.K., in 1994. He is currently a Professor of Power Systems Engineering, University of Portsmouth, U.K. Between 1989 and 1991, he was an Electrical Engineer at C.V.G. Edelca, Caracas, Venezuela. Between 1994 and 1999, he was a Post doctoral Research Fellow at the Control Engineering Research Centre, City University. Between 2000 and 2015, he was an academician with the School of Systems Engineering, University of Reading, Reading, U.K. His research interests include a range of issues related to electrical power systems, as well as the methods and applications of automatic control, and also include control of power systems, energy storage and its integration to power grids, computational intelligence for smart grids, optimal control, nonlinear control, state estimation and robotics. Professor Becerra has received research funding during his career from the

## 1. INTRODUCTION

Performance degradation in most mechanical systems with contacting surfaces in relative motion is often due to the phenomenon of friction. This could be manifested for example as a deterioration in the tracking error, limit cycle oscillation, or stick-slip motion (Dupont and Dunlap, 1995) and (Grami and Gharbia, 2017). Previous studies on friction have revealed two distinct regimes known as pre-sliding and gross-sliding. The pre-sliding regime friction is the friction experienced by a system from the time of application of an external force up until the surfaces are on the verge of sliding relative to each other. When the applied external force is large enough to break the adhesive forces between the surfaces in contact, the gross-sliding regime is initiated and there is relative motion between the surfaces. Hence, the friction force associated with the gross-sliding regime is the one that occurs when the contacting surfaces are moving relative to each other, and is a function of the relative velocity of motion between these surfaces.

Friction is a non-linear complex phenomenon (Saleem, Al Ratrout and Wong, 2017) with varied dynamics governing the pre-sliding and gross-sliding regimes and, as a result, although various efforts have been made to model friction, it has been challenging to obtain a generally accepted model that is reasonably simple to implement and yet captures all the key features of the friction phenomenon. This is due to the complex and dynamic nature of friction with regime dependent characteristics. The key features of friction include non-drift property, hysteresis with non-local memory characteristics, stick-slip motion, frictional lag and Stribeck effect. Friction models presented in literature range from the simple static models such as the Coulomb model and its variants (Reynolds, 2014), the Stribeck model (Geffen, 2009) to the dynamic friction models, such as the bristle (Haessig and Friedland, 1991), Dahl (Dahl, 1968), LuGre (Canudas de Wit *et al.*, 1995), Elasto-plastic (E-P) (Dupont *et al.*, 2002), GMS (Lampaert, Al-Bender and Swevers, 2003) and Xiong (Xiong, Kikuuwe and Yamamoto, 2012) models. Some of the more prominent friction models in the control area would be further analyzed and compared in the proceeding section with the proposed new model.

These models vary in their complexity and ability to predict friction dynamics (Armstrong-Helouvry, Dupont and Wit, 1994) with the static models being simpler in structure though unable to capture dynamic phenomena such as frictional lag and pre-sliding hysteresis. This is because they are usually modeled as a function of the velocity only. The dynamic models, on the other hand, vary in their complexity and thus the ease with which they capture friction dynamics both in the pre-sliding and gross-sliding regimes. These dynamic models, often a function of both the displacement and velocity capture friction dynamics though to varying

degrees. A more detailed review of these and other friction models is further provided in (Armstrong-Helouvry, Dupont and Wit, 1994), (Geffen, 2009) and (Nnaji, 2017).

The twin issues of model fidelity, and ease of implementation and model parameter estimation are of great importance in the field of control. As such most models are judged based on how closely they satisfy these key issues. The popular LuGre model is very simple to implement due to its low number of parameters. However, for high precision systems its behavior does not reflect true system friction in the pre-slide regime. On the other hand the Generalized Maxwell Slip model predicts true system friction both in pre-slide and gross-slide regimes. However, its structure is such that it uses many parameters (being multi-element in nature) for prediction. This makes implementation difficult. Thus these models and their variants as further discussed in section 2 do not satisfy the objectives of model fidelity and ease of implementation. The motivation for this research paper is predicated therefore on the need to present a friction model that meets the above stated objectives in all regimes of friction.

The model presented in this paper is suitable for predicting friction features for both the pre-slide and gross-slide regimes. The number of model parameters are also low comparable to the LuGre model thereby making it easy to estimate and thus implement. As a result the proposed model could readily lend itself to be used in model-based friction compensation schemes. Results of various experiments performed on a friction test-bed showed that the proposed model exhibits superior correspondence with real friction than the LuGre and GMS models in terms of the mean square error (MSE) measures.

The layout of the rest of the paper is as follows; in section 2 a novel friction model which exhibits hysteresis with non-local memory is presented in addition to describing other well-known friction models. Section 3 demonstrates the proposed model's capability for predicting relevant friction features such as the stick-slip motion, Stribeck effect, friction hysteresis and non-drift properties through simulations. Section 4 describes friction characterization experiments on a friction test-bed designed for the purpose. This is followed by system identification and model validation in section 5. The results of the system identification and models validation are discussed in section 6. Finally, section 7 provides concluding remarks.

## 2. FRICTION MODELS

Static friction models such as the classical models do not capture relevant friction dynamics and may not be adequate for high precision control systems design. On the other

hand, dynamic friction models though able to capture many of these dynamics are generally more complex and this complexity increases with increasing dynamics of the friction model. This scenario results in the trade-off between model fidelity and simplicity which are key objectives in system modeling and control. Thus a good model is not necessarily judged only by its ability to replicate friction features but also by the ease with which such models could be used for their desired objectives such as simulation and/or control. In this section a review of the LuGre and GMS models are presented providing the background for the new model presented thereafter.

### 2. 1 The LuGre friction model

The LuGre friction model proposed in (Canudas de Wit *et al.*, 1995), has become one of the most popular models of friction in the control area and thus is worth reviewing in this paper. The LuGre friction model gained much popularity because of its low number of parameters (6) which are easy to identify using system identification methods and the integration of both regimes of friction in a single differential equation. The LuGre model is formulated thus from the Dahl model as

$$F_f = \sigma_0 z + \sigma_1 \dot{z} + f_v v \dots \dots \dots \dots \dots 1$$

$$\dot{z} = v - \sigma_0 \frac{|v|}{g(v)} z \dots \dots \dots \dots \dots .2$$

$$g(v) = F_c + (F_s - F_c)e^{-\left(\frac{v}{v_s}\right)^2} \dots \dots \dots \dots .3$$

where $F_f$ is the friction force, $f_v$ the viscous damping coefficient, $z$ the micro displacement between the surfaces (or bristle deflection), $\sigma_0$ is the stiffness of the material, $\sigma_1$ is the material damping coefficient, $g(v)$ is the non-linear term modeling the Stribeck effect at low velocities, $F_c$ is the Coulomb (kinetic) friction force, $F_s$ is the static friction force (the minimum amount of force required to initiate relative motion between the two bodies in contact), $v$ is the relative velocity between the surfaces in contact and $v_s$ the Stribeck velocity.

The model has widely been used in pneumatics, robotics and mechanical systems for the compensation of systems with friction, (Lu *et al.*, 2009), (Guenther *et al.*, 2006; Khayati, Bigras and Dessaint, 2009). Despite this popularity the LuGre friction model has been observed to have some limitations such as:
- Inability to accurately reproduce experimentally observed reversal point with non-local memory at pre-sliding displacements (Altpeter, 1999; Swevers *et al.*, 2000).
- Being subject to positional drift at small displacements in the pre-sliding regime (Dupont, Armstrong and Hayward, 2000; Al-Bender, Lampaert and Swevers, 2005).

To overcome the positional drift of the LuGre model, the elasto-plastic (E-P) friction model was proposed in (Dupont *et al.*, 2002). However this model does not solve the non-local hysteresis problem associated with the LuGre model. Because of the close relation between the LuGre and the E-P models, a review of the E-P model is not described further in this paper.

### 2. 2. The Generalised Maxwell Slip (GMS) friction model

The GMS friction model (Lampaert, Al-Bender and Swevers, 2003) is a multi-element, multi state model unlike the LuGre which is single state. As such it can also be regarded as a multi- model representation of the friction phenomenon (Zhao and Zhang, 2019). Two different sets of state equations describe the pre-slide and gross-slide regimes of friction. In the pre-slide stick regime

$$\dot{z}_\iota = v \dots \dots \dots \dots \dots \dots \dots \dots \dots 4$$

and for gross-slide slip regime

$$\dot{z}_\iota = sgn(v)C_i\left(1 - \sigma_{0i}\frac{z_i}{g_i(v)}\right) \dots \dots \dots \dots 5$$

$$i = 1, 2, \dots \dots, N$$

During stick, the elements remain stuck till the deflection $z_i = \frac{1}{z_{0i}}g_i(v)$, and also during slip, the element continues to move until the velocity v goes through zero (reversal). The friction force is thus given as;

$$F_f = \sum(\sigma_{0i} + \sigma_{1i}\dot{z}_\iota) + f_v v \dots \dots \dots \dots 6$$

where $z_i$ is the deflection of the ith element, $g_i(v)$ is the velocity weakening Stribeck function, $C_i$ is an attraction parameter showing how rapidly the $z_i$ tracks changes in $g_i(v)$, $\sigma_{0i}$ is the stiffness of the ith element and N is the number of massless bristle elements. The GMS model is capable of modelling most friction features including the pre-sliding friction hysteresis with non-local memory and it does not exhibit position drift as does the LuGre model. The applicability of this model is however limited due largely to difficulties in implementation and parameter estimation. This is because of the large number of parameters needed to capture friction features accurately (Xiong, Kikuuwe and Yamamoto, 2012). Similar to the GMS model is the Xiong model, the difference lies with the realization of the pre-slide and gross slide friction regimes of friction. The number of parameters are similar and difficult to identify and implement (Xiong, Kikuuwe and Yamamoto, 2012). In table I, some dynamic models of friction such as the LuGre, Elasto-Plastic (E-P), GMS and Xiong models are presented and compared in terms of their ability to model important friction features such as nonlocal memory hysteresis, Stribeck effect and non-drift property, and also the ease of their parameter identification and implementation. From the

table 1, the LuGre and E-P models are not able to accurately capture non-local memory hysteresis features of friction. The E-P model does not exhibit positional drift but the LuGre model does. On the other hand, the GMS and Xiong models though able to capture more accurately the pre-slide hysteretic features with non-local memory, they require a large number of parameters thus making identification and implementation challenging (Xiong, Kikuuwe and Yamamoto, 2013). Identification of parameters becomes increasingly difficult as the number of parameters increases. This is partly the reason the LuGre model is more popular among control experts despite its drawbacks.

## 2. 3. The novel friction model

The friction phenomena is such that the pre-sliding and gross sliding friction features differ and hence would require different model features to capture these behaviors. Thus a model structure proposed to capture hysteresis friction features in the pre-sliding regime is

$$F_{hyst}(z) = f_b(z) + f_r \dots\dots\dots\dots\dots\dots 7$$

with

$$f_b(z) = \sin\left(\frac{z}{|z_t - z_r|}\frac{\pi}{2}\right)|f_t - f_r| \dots\dots\dots\dots 8$$

where $F_{hyst}(z)$ is the total friction force in the pre-slide regime at any given time, $f_b(z)$ is the branch friction function, z the bristle displacement, $z_r$ the displacement at the beginning of branch motion (accounting for the state of the bristles prior to force application), $z_t$ is the target displacement (which depends on breakaway $Z_b$ displacement value), $f_r$ is the friction force at the beginning of a branch motion (this takes into account the stressed state of the bristles), $f_t$ target friction force (this depends on the stiction force ($F_s$). The term $z_t$ is further expressed in terms of the breakaway displacement and the bristle position at the beginning of a new branch as $2Z_b$- $z_r$ for $z_r \neq 0$ and $Z_b$ for $z_r = 0$ (no initial deflection of the bristle). Likewise $f_t$ can be further expressed in terms of the breakaway (stiction) force and the force at the beginning of a new branch as $2F_s$- $f_r$ for $f_r \neq 0$ and $F_s$ for $f_r = 0$ (non-stressed state of the bristle). Thus the breakaway displacement $Z_b$ parameter indirectly appears in the equation for pre-slide, see eqn. 8. The proposed friction model structure for both regimes of friction, obtained by substituting eqn. 7 into eqn. 1 of the LuGre model becomes

$$F_f = F_{hyst}(z) + \sigma\dot{z} + f_v v \dots\dots\dots..9$$

Two state equations introduced are

$$\dot{\gamma} = \frac{g(v) - \gamma}{\tau} \dots\dots\dots\dots\dots\dots 10$$

and

$$\dot{z} = \frac{1}{\sigma}\left(sat\left(\gamma, F_{hyst}(z) + \sigma v\right) - F_{hyst}(z)\right)..11$$

with $g(v) = F_c + (F_s - F_c)e^{-\left(\frac{v}{v_s}\right)^2}$
known as the Stribeck function, same as eqn. 3

where $v_s \neq 0$, is the Stribeck velocity (a velocity threshold above which the Stribeck curve slope changes from negative to positive), $\gamma$ is a state variable representation of the lagged version of the Stribeck function $g(v)$. It was introduced to improve the frictional-lag prediction capability of the model (Xiong, Kikuuwe and Yamamoto, 2012), $\tau$ is the time constant (delay), it determines how fast the new state variable tracks $g(v)$, z is the average bristle deflection, $F_{hyst}(z)$ is the pre-sliding friction force, $\sigma$ is the material damping coefficient( micro-viscous damping parameter), $v$ is the relative velocity of the bodies in contact, $f_v$ is the viscous damping coefficient (macro-viscous friction component), and $F_f$ is the overall friction force. Important properties of this proposed friction model such as dissipativity, continuity and boundedness are demonstrated in (Nnaji, 2017) and are not discussed further in this paper. The friction models equations described above are all for translational motion, but can be converted to their rotational equivalents by simple substitution of relevant translational parameters with rotational parameters.

## 3. DYNAMIC FEATURES OF THE NEW FRICTION MODEL

Ability of the proposed friction model to predict friction features in the pre-sliding and gross-sliding regimes are demonstrated through simulations and validated by experiments. Some of these features are; pre-sliding hysteresis with non-local memory, the non-drift property, stick-slip motion, Stribeck effect and frictional lag. A simple mass-spring mechanical system shown in figure 1 was used to perform the friction features simulations described below. The parameter values used in the simulations that follow were chosen from a series of friction experiments performed in the laboratory using the friction test-bed while the stiction force, Coulomb friction and micro-damping values were chosen for simulation purposes in agreement with (Canudas de Wit *et al.*, 1995) and (Olsson, 1996) for comparison with other models. The table 2 shows the parameters used for the simulation of the various friction features of the new friction model.

### 3. 1 Pre-slide behavior

First we simulate real friction behavior for an applied force of less value than the stiction force (Fs) to capture the pre-slide friction hysteresis, and then the non-drift property of actual friction behavior in real systems using the proposed model of friction.

*Friction hysteresis*; This is the friction feature arising from the adhesion and deformation of the surface asperities when subject to external force leading to an elastic-plastic behavior of the asperities. These interactions give rise to friction force dependent on the relative displacement of the asperities rather than the relative velocity of the contacting bodies (Drincic, 2012). This rate independent friction feature also exhibits a non-local memory feature which

implies that future development of such a system depends on past history of states and does not fade. Such systems are thus said to have memory. Simulation of hysteretic feature of friction in the pre-slide regime with nonlocal memory characteristics using the novel friction model is shown in figure 2b for a certain reference displacement figure 2a of lower value than the minimum required for relative motion of the contacting bodies. During the pre-slide regime, the friction force is captured by the pre-slide friction function given by equation 7. This hysteresis figure 2b is different from that captured by the LuGre model (Canudas de Wit *et al.*, 1995). Therefore the LuGre and E-P models are not able to effectively capture this important feature of friction in the pre-slide regime (Altpeter, 1999) and (Geffen, 2009). The GMS and Xiong models can model this feature though with large number of parameters thus making implementation expensive.

*Non-drift property*; Non-drift feature simply means that if the applied force is smaller than the stiction value there is no resultant displacement between the two bodies in contact. Thus the contacting bodies do not move relative to each other at such times (Al-Bender, Lampaert and Swevers, 2005). Real friction does not exhibit drift in the pre-slide as a result of forces less than the stiction value. In performing the simulations the force input used is shown in figure 3a, and the system is a simple mass with friction subjected to an external force, figure 1. The force input initially ramps to a value much greater than the stiction and then suddenly falls well below this value and remains below stiction while moving in a zig-zag manner. Interest is on the ability of the model to predict the non-drift feature of real friction between contacting surfaces when the applied force is less than the static friction force.

On simulation, the new model captured the stiction force and subsequent motion till the force falls below the stiction level. In the region where the force is less than the stiction force, friction is virtually equal to the applied external force as shown in the plot of figure 3b. One easily notices the hysteresis loop in the friction-position plot also. The figure was truncated to enhance the area of interest which is the region where the force is well below the stiction force. The exhibition of the non-drift feature is seen as a hysteresis loop whose displacement value does not increase under the applied force so long as it remained below the stiction value. In the same vein the LuGre model exhibits positional drift in the pre-slide regime as reported in (Dupont *et al.*, 2002). The E-P, GMS and Xiong models show non-drift friction property (Al-Bender, Lampaert and Swevers, 2005).

### 3. 2.  Gross-slide behavior

Next we simulate gross-sliding friction force features such as the stick-slip motion, Stribeck effect and frictional lag using the proposed friction model.

*Stick-slip motion;* This is described as the intermittent sticking and sliding periods between two surfaces under an external force due to the spring-like nature of friction between the two bodies. This causes systems experiencing stick-slip to have periods of motion when the external force is greater than the stiction followed by periods where the relative motion becomes zero (stick) when the stiction force becomes greater than the external force and the system behaves in spring-like manner (Desrayaud *et al.*, 2013). As stated earlier, stick-slip effect is one of the negative effects as a result of friction non-linearity affecting the low velocity regimes. The friction force modeled by the proposed model captures the stick-slip friction effect at low velocities as in figure 4a. The position plot shown in figure 4b indicates periods of slip (gradient) and stick (horizontal). The stick-slip motion is often treated together with the Stribeck effect in some literature because of their close relationship, however, in this paper they are separately treated for clarity and emphasis.

*Stribeck effect and frictional lag*: Stribeck effect is the feature of friction resulting in the non-linear decrease in the friction value as velocity increases from zero. This feature depicts a static relation between friction force and velocity. Many researchers have documented these features as predicted by some relevant models of friction like the LuGre, GMS and Elasto-Plastic models (Lampaert, Al-Bender and Swevers, 2003), (Dupont, Armstrong and Hayward, 2000). The focus was on how the proposed model is able to predict this friction feature (Stribeck effect). In carrying out the simulations the default parameters value were used as for the stick-slip simulation. The velocity input signal was incremented from zero to 0.45m/s. Figure 5 portrays the friction force in relation to the velocity input. This feature, known as the Stribeck effect shows the friction force decreasing from the static value (breakaway friction force) towards its minimum Coulomb (kinetic) friction value for increasing velocities.
This plot of the friction force at low velocities is called the Stribeck curve.

The proposed model was also able to model friction for varying unidirectional velocities also known as frictional lag. The frictional lag effect is an experimentally observed friction feature showing the variation of friction for increasing velocities (acceleration) and decreasing velocities (deceleration). This feature of friction as captured by the novel friction model is further explained in section 4.2.3 and figure 10 c, using experimental results.

*Breakaway and varying breakaway friction:* Increasing the applied external force to the system of figure 1 will lead to a friction force build up. This build up will continue proportionately with the externally applied force until it is able to break the forces of adhesion between the two surfaces to initiate a relative motion between them. The friction force value beyond which the bodies slide relative to each other is termed the breakaway (stiction) force and it has been experimentally found that this value is dependent on the rate at which the force is being applied (Rabinowicz, 1958).

For the varying breakaway force feature, a ramp force signal was used varying the slope (rate) to achieve time varying force application as follows: 0.1N/s, 0.05N/s, and 0.2N/s, the effect of force rate variations on the breakaway friction force as predicted by the proposed model is depicted in figure 6. From the figure one notes that increasing the rate at which the force is increased increases the breakaway friction force.

Thus the model predicts the breakaway variation showing that as the rate of application of the external force is increased, the breakaway friction force predicted also increased, figure 6. From the figure the breakaway friction force values for the different force rates; 0.05N/s, 0.1N/s and 0.2N/s are respectively 1.491N, 1.498N and 1.499N.

## 4. FRICTION CHARACTERIZATION EXPERIMENTS

In the previous section, prediction of relevant friction features using the proposed model was demonstrated through simulations. A series of experiments were performed on a friction test-bed for the characterization of friction phenomena, system identification and model validation. A brief description of the friction test-bed, the various experiments carried out and procedures are presented in this section.

### 4. 1 Experimental set-up (test-bed)

The set-up of the experimental friction test-bed is as shown in figure 7a, it consists of an SRV-02 rotary servo in the high gear ratio driving a load through an external gear system. Friction occurs in the motor shaft, gear transmission system, and friction load-discs in the system. Friction between the load-discs being larger than the others. A data acquisition card (Q2-USB) was used as interface between the hardware (friction test-bed) and the MATLAB/SIMULINK based real time software used to drive the system running on a PC in a Hardware-In-the-Loop (HIL) manner.

The quadrature encoder reads the angular position of the load while the tachometer measures the motor angular speed. The SIMULINK provides a platform for command inputs and implementation of control strategies on the test-rig. A universal power supply module supplied DC power to drive the motor, while another DC source provided excitation for the friction torque sensor. During operation the torque between the fixed load disc and the rotary disc attached to the output shaft of the gear was measured by the torque sensor attached to the fixed load-disc.

### 4. 2 Procedure

A brief description of the various characterization experiments performed using the laboratory friction test-bed is first presented in this section alongside the results of such experiments. The different input signals for the experiments

were so designed so as to capture the various features of the friction phenomena especially the in the pre-slide and gross-slide friction regimes.

*Constant velocity experiment;*
Previous researches indicate that at very low velocity ranges the friction curve has a negative slope for velocity increments (Stribeck, 1902). However, beyond the velocity threshold called the Stribeck velocity, the friction-velocity relation becomes more linear and positively sloped. This behavior is thus termed the Stribeck effect. A closed loop (velocity feedback) approach was adopted in the series of constant-velocity experiments to take advantage of its appeal and merits over the open loop. A series of constant velocities were then introduced into the system and the resultant friction torque measured using the torque sensor. The velocity and torque values were recorded. The reference velocities for the experiment range from very low values of 0.003 0 rad/sec-to-1 rad/sec incremented by 0.003 rad/sec. For each velocity 10 experimental runs were performed and the average value of the corresponding torque obtained. This is to improve result accuracy. Thus the friction torque-velocity data points was obtained and used for the friction identification.

A different set of experiment was performed using interval of similar velocity range as the previous but with an interval of 0.005 rad/sec for model validation purposes. The results of the constant velocity friction experiments are shown in figure 8 as red dots.

*Pre-sliding experiment;*
The pre-sliding hysteresis with non-local memory has been established as against the non-memory based behavior earlier believed to govern the pre-sliding regime (Dhaouadi and Ghorbel, 2008). This characteristic feature of friction is independent of the relative velocity of the bodies in contact indicative of the predominance of the elastic deformation characterizing the bristles behavior in this regime. The experiment to determine this relationship friction has with displacement was performed in two stages as follows;
Stage 1: A displacement signal variable was injected into the system with slow increments until the time gross-sliding was initiated and the surfaces moving relative to each other. This process was repeated 10 times and the average friction torque and the corresponding displacement input were recorded thus giving a range of values for which the system was in the pre-slide condition and that beyond which a relative motion was observed. The value of the pre-sliding displacement was also obtained to determine a range of values for the pre-sliding displacement before breakaway.
Stage 2: A special input position signal shown as figure 2a was then used ensuring the Stiction torque as earlier determined in stage 1 above was never exceeded by the signal input. The measured friction torque from the experiments is shown in figure 9a. The result exhibited some quantization due to the fact that the range of the torque-sensor used for the measurement is large compared

to the actual friction signals measured in the pre-slide regime experiments.

*Frictional lag experiment;*
There is a relative time-lag between the friction torque and the corresponding velocity, in the sense that the system friction does not change instantaneously as velocities change. This lag gives rise to a hysteresis effect in the gross-sliding regime similar to the hysteresis effect in the pre-sliding regime. Research (Hess and Soom, 1990) shows that the frictional torque is larger for increasing velocities (acceleration) than for decreasing velocities (deceleration), the loop of the frictional lag encloses the Stribeck low velocity curve indicative of the vanishing of the former for increasing velocities (Al-Bender, Lampaert and Swevers, 2004). In designing the experiment, a time varying periodic unidirectional reference signal was applied. This was to ensure adequate capture of the low velocity variations as a function of time. To achieve this a sinusoidal velocity signal of the general form shown as eqn. 12 was used.

$$v(t) = A + Bsin(\omega t) \dots \dots \dots .12$$

where A is a positive bias velocity signal chosen in such a way as to ensure the velocity is always unidirectional ie $|A| > |B|$, $\omega$ is the angular velocity between the surfaces and t is time. The values of $\omega$ are: 2, 5, 10 rad/sec and a chirp signal. For the experiments the values used are; B = 0.95, and A = 1, thus the periodic velocity becomes

$$v(t) = 1 + 0.95sin(\omega t) \dots \dots \dots .13$$

Various angular velocities of $\omega$ = 2, 5 and 10 rad/sec, were used to run the experiment and their data sets recorded. Identification and validation data sets were collected from two separate experiments to be used in the next section. The data set for the validation was based on a system with frequency of 5 rad/sec while the identification data was based on a chirp signal with a frequency range up-to 10 rad/sec. The results so obtained is shown as figure 10, blue color.

1. **SYSTEM IDENTIFICATION AND VALIDATION**

## 5. 1 Identification

System identification requires that the input and output measurements from the experiments on the test-bed be obtained, a suitable model structure is then chosen and then an estimation approach adopted to estimate the model parameters. In this case the results of the characterization experiments reported in the previous section are used as the input_output data set in an offline manner, while the proposed friction model structure was chosen for parameter estimation. Model parameters estimation for the LuGre and GMS model structures are also discussed in this section followed by model validation.

For simplicity the estimation of the various parameters of the proposed friction model was split into 2 namely;

static parameter estimation and dynamic parameter estimation.

### 5.1. 1 Estimation of the static parameters
The static parameters to be estimated are;
$F_c$ (N) is the Coulomb friction parameter
$F_s$ (N) is the stiction friction parameter
$f_v$ (Ns/m) is the viscous friction coefficient parameter
$v_s$ (m/s) is the parameter representing the Stribeck velocity

In the gross-slide regime, the state equation 11 becomes
$$\sigma \dot{z} = \gamma - F_{hyst}(z)$$
For steady state the state equation 10 reduces to
$$\gamma = g(v)$$
Substituting these into equation 9, the proposed friction model is thus given as
$$F_f = g(v) + f_v v \dots \dots \dots .14$$
Since $g(v)$ is given as equation 9 thus equation 14 becomes

$$F_f = F_c + (F_s - F_c)e^{-\left(\frac{v}{v_s}\right)^2} + f_v v \dots \dots \dots \dots \dots 15$$

Therefore the proposed friction model is same as the Stribeck equation of equation 3 in the steady state.

If the torque output data set obtained from previous experimental measurements is $Y(t)$, and the velocity input data set as recorded by the tachometer is $U(t)$, then the input-output data set is represented as

$$\phi(t) = [U(t), Y(t)]^T \dots \dots \dots \dots \dots 16$$

with
$$U(t)^T = [u(t-1), u(t-2), \dots, u(t-n)]..17$$
and
$$Y(t)^T = [y(t-1), y(t-2), \dots, y(t-1-n)]..18$$
where $\phi(t)$ is a vector of the input and output data set, $U(t)$ is the vector input data and $Y(t)$ the scalar output data. Therefore the objective is to obtain estimates for the mathematical relationship between the input-output data sets so as to enable the prediction of current values from past observations. We thus define this relationship as
$$y(t) = \phi(t)^T \theta + e(t) \dots \dots \dots \dots \dots 19$$
The error equation therefore becomes
$$e(t) = y(t) - \phi(t)^T \theta \dots \dots \dots \dots 20$$
with $y(t)$ as the measured friction-torque output, $\phi(t)^T \theta$, a non-linear function defining the model structure, is called the regression vector, $\theta$ is the vector of parameters to be identified, $e(t)$ being the error term added to account for the fact that the output is no perfect function of the past input-output data set. The goal is to ensure the contribution of the error term is infinitesimal so as to reasonably say that for a given past data set, the current output $y(t)$ is accurately predicted by the model structure so chosen.
For the steady state optimization, the model structure is given as

$$\phi(t)^T \theta = F_c + (F_s - F_c)e^{-\left(\frac{v}{v_s}\right)^2} \dots \dots \dots \dots 21$$

here the vector of parameters $\theta$ consists of the static parameters namely; $F_s$, $F_c$ and $v_s$.           Various approaches have been adopted for the identification of the static parameters, (Bai, 1997; Al-duwaish, 1999; Xiang, Qiu

and Li, 2009). This kind of identification problem usually gives rise to a non-linear regression between the chosen model and the data-set as shown below. Substituting equations 21 into 20 gives rise to an error equation whose cost function $C$ is described as equation 22.

$$C = \sum_{t=1}^{N} \| y(t) - \phi(t)^T \theta \|^2$$

with N being the number of data-points in the data-set, $C$ the cost function, and every other term as previously defined. The objective is thus the minimization of the cost function $C$. This therefore reduces the identification problem to a quadratic curve-fitting problem of the data set using an optimization tool. The parameter values obtained for the system after optimization is shown in table 3 with the Mean Square Error (MSE) value of the estimation. The graph of the modelled friction-torque against the velocity variable for the proposed model is shown as figure 8a (blue color), using the identified model parameters. The graph of the optimization result shows the general behavior of friction capturing the Stribeck effect and the linear viscous plus Coulomb friction. To obtain a parsimonious friction model which best models the friction velocity relationship at steady state velocities a validation of the proposed model structure representative of friction in the regime would be performed in the proceeding section.

### 5.1. 2 Estimation of dynamic parameters

The dynamic parameters for identification are the breakaway displacement $Z_b$ (m), micro-damping $\sigma$ (Ns/m) and the lag parameter $\tau$ (s). The approach adopted for estimating these parameters are explained separately below.

***Estimating the Breakaway displacement*** $Z_b$: In the pre-slide regime the parameters of interest for the proposed model are the stiction torque $F_s$ and the breakaway displacement $Z_b$. However, the stiction torque obtained from the previous subsection 5.1 was used. Hence, the identification focused only on the breakaway displacement $Z_b$. The proposed model equation for the pre-sliding friction regime is

$$F_f = F_{hyst}(z) + \sigma \dot{z} \dots \dots ..23$$

with

$$\sigma \dot{z} = v \dots \dots \dots 24$$

$z$ is the average bristle deflection, and $\sigma$ the micro-damping parameter and $v$ the relative velocity. Using a slowly varying input signal makes it possible to neglect the dynamics (Altpeter, 1999). Therefore equation 23 becomes

$$F_f = F_{hyst}(z)$$

with

$$F_{hyst}(z) = \sin\left(\frac{z}{|z_t - z_r|}\frac{\pi}{2}\right)|f_t - f_r| + f_r \dots \dots 25$$

being the pre-sliding friction function. Considering a small range in the region of the pre-slide regime therefore, equation 25 becomes

$$F_{hyst}(z) = \left(\frac{z}{|z_t - z_r|}\frac{\pi}{2}\right)|f_t - f_r| + f_r$$

Recall that $z_t = 2Z_b - z_r$ and $f_t = 2F_s - f_r$ (section 2.3). Substituting these relations into this equation, the regression vector becomes

$$\phi(t)^T \theta = \left(\frac{z - z_r}{|Z_b - z_r|}\frac{\pi}{2}\right)|F_s - f_r| + f_r \dots \dots 26$$

Thus the identifiable parameters from equation 26 are 2; the breakaway displacement $Z_b$ and the breakaway friction torque $F_s$. Thus the cost function is

$$C = \sum_{t=1}^{N} \| y(t) - \phi(t)^T \theta \|^2 \quad \dots \dots \dots 27$$

Minimization of the cost function $C$ of equation 27 was done using a non-linear optimization tool for the identification of the breakaway displacement parameter $Z_b$. The MSE values is given in table 4, while the predicted friction-torque features against the true hysteretic friction is shown in figure 9a (red color).

***Computation of the dynamic parameter*** $\sigma$: From previous identification approaches it was possible to estimate most of the parameters of the novel friction model with the exception of the micro-damping parameter $\sigma$ There has been no straight forward approach for estimating the micro-damping parameter, however many techniques have been adopted in literature for its computation from experimental results as demonstrated in (Al-duwaish, 1999), (Vargas, De Fieri and Castelan, 2004). The experiment for the computation of this parameter was performed in the pre-slide friction regime with a slowly varying ramp input signal of small range as suggested in (Vargas, De Fieri and Castelan, 2004). Thus within this range, a linearized model of the pre-sliding hysteresis function was used to compute the $\sigma$ parameter value. The linearized version of the pre-sliding equation is

$$F_{hyst}(z) = \left(\frac{z - z_r}{|Z_b - z_r|}\frac{\pi}{2}\right)|f_t - f_r| + f_r \dots 28$$

with $f_t = z_r = 0$ for motion starting from rest, $Z_b = z_t$ and $F_s = f_t$.
Therefore,

$$F_{hyst}(z) = \frac{F_s \pi}{2Z_b} z \dots \dots \dots \dots ..29$$

For the system test-bed, with a second order Laplace representation as

$$Js^2 z = u - F_f \dots \dots \dots \dots \dots .30$$

where $u$ is the control input, $F_f$ being the pre-slide friction function given in equation 29 as $F_{hyst}(z)$ and $J$ the moment of inertia of the system. Substituting this value of $F_f$ into equation 30 gives the forward transfer function G(s) of the test-bed to be

$$G(s) = \frac{1}{Js^2 + (\sigma + f_v)s + \frac{F_s \pi}{2Z_b}} \dots \dots \dots .31$$

Thus the transfer function equation 31 is characterized by second-order dynamics with undamped natural frequency $\omega_n$ and a damping ratio $\zeta$.
A damping ratio $\zeta$ such that $0.5 \leq \zeta \leq 1$ ensures adequate damping of the system, here a value of $\zeta = 0.7$ was chosen. Comparing equation 31 with the standard second order

transfer function, the micro-damping parameter could be determined (Nnaji, 2012). Thus from equation 31 above

$$\sigma + f_v = 2J\zeta\omega_n \ldots\ldots\ldots\ldots\ldots\ldots.32$$

with

$$\omega_n^2 = \frac{F_s\pi}{2JZ_b}$$

Substituting this value into equation 32 yields

$$\sigma = 2\zeta\sqrt{\frac{JF_s\pi}{2Z_b}} - f_v \ldots\ldots\ldots\ldots\ldots\ldots 33$$

Given $F_s$, $Z_b$ and $f_v$, obtained in the previous estimation as 0.0994, 0.0060, and 0.0403 respectively while the equivalent moment of inertia $J$ of the system used is $6.528\text{x}10^{-5}$, then $\sigma = 0.0174$.

***Estimation of the lag parameter $\tau$***: At low to medium unidirectional velocities, the friction feature depicts a lag between the friction torque and the corresponding velocity. The friction model structure for the gross-sliding regime is used for the $\tau$ parameter estimation purposes. In the gross sliding regime the state equations 11 and 10 are

$$\sigma\dot{z} = \gamma - F_{hyst}(z) \ldots\ldots\ldots\ldots\ldots.34$$

and

$$\dot{\gamma} = \frac{g(v) - \gamma}{\tau} \ldots\ldots\ldots\ldots\ldots\ldots.35$$

Substituting these into the friction torque equation 9 yields

$$F_f = \gamma + f_v v \ldots\ldots\ldots\ldots\ldots.36$$

From these equations (equations 36 and 35), it is clear that the static parameters in $g(v)$ appear here as well, however they were determined in the constant velocity estimation in section 5.1. The estimates earlier obtained from the constant velocity identification were adopted in the present estimation hence the major focus is the identification of the lag ($\tau$) parameter. The predicted frictional-lag features are shown in figure 10a (in red color), while the estimated parameter values and the MSE are recorded in table 4.

The width of the frictional torque has been shown by many researchers (section 3) to widen or shrink as the velocity rate (i.e. acceleration) increases or decreases respectively. This phenomenon is called frictional-lag.

The friction-torque for various unidirectional sinusoidal velocity inputs were plotted using the estimated parameters of the proposed model and is shown in figure 10c. This clearly illustrates that the friction-lag feature widens as the angular velocity increases. The following angular velocities; 2 rad/sec, 5 rad/sec and 10 rad/sec were used for this experiment (section 4). This thus demonstrates the ability of the novel friction model to predict frictional-lag. The values for all the parameters of the novel friction model as estimated from the various experiments described above is as shown in table 5. These values exhibited excellent correspondence with experimental friction dynamics obtained from the laboratory friction test-bed. In the same manner estimation of the static and dynamic parameters for both the LuGre and GMS friction models were performed and the MSE compared with the proposed model.

To accomplish this the friction data set obtained for the various characterization experiments carried out in section 4 with the various inputs were used for the system identification of the parameters of the GMS and LuGre models. Table 6 shows the prediction comparison of the three models for gross-sliding friction regime namely the Proposed, LuGre and GMS models in terms of their Mean Square Error value (MSE) for both estimation and validation. In the same manner, prediction performance of the three models in the pre-slide friction regime namely friction hysteresis with non-local memory was presented in table 7.

### 5. 2 Model validation

A carefully selected set of experiments were performed and the data set were used for the validation of the new friction model structure. The same set of experimental data were used for the validation of the LuGre and GMS models discussed earlier for the purposes of comparison. The purpose of model validation was to determine how well the estimated model parameters represent true system friction as exhibited by the laboratory friction test-bed. For simplicity, the approach adopted closely resembled the system identification approach of splitting the validation process into the constant-velocity, pre-sliding hysteresis, and the frictional-lag procedures thus capturing friction behavior in these regions using the novel friction model, LuGre and GMS friction model structures against the experimental results. Data sets used for the validation exercise were different from those used for system identification.

***Constant velocity***

The proposed novel friction model was validated against a set of constant velocity friction experiment data different from the one used for the identification. The experiment was performed similar to that for friction identification. The performance of the model with its parameters as obtained from system identification section 5.1, tabulated in table 5 was compared against the validation experiment data set (in red dots) and the model prediction result (in blue line) plotted as figure 8b. From the figure 8, the proposed model behavior showed strong correlation with the experimental data. The validation MSE for the proposed model is recorded in table 3. This was also done for the LuGre and GMS models.

***Pre-sliding hysteresis***

The behavior of the friction model with parameter values as shown in table 5 in the pre-sliding regime against the friction-torque data set (blue line) obtained from a set of experiments performed for the purpose of validation using a sinusoidal input displacement variable is shown in figure 9b (red color). The figure showed that the proposed model performance is in close agreement with the validation experiment data-set. This underscores the ability of the model to capture non-local features of the relationship between friction and displacement in the pre-slide friction regime efficiently. In the same way LuGre and GMS models

were also used for validation and the result is shown in table 6.

### Frictional lag

Using the obtained parameter values for the proposed friction model of table 5 alongside the validation data set (blue line) generated by performing a frictional lag experiment using a 5 rad/sec unidirectional sinusoidal velocity input, the model performance against the validation data set was captured in figure 10b (in red). The error measure (MSE) was recorded in table 4 showing a strong correspondence.

### 6. DISCUSSION

The results of the various friction characterization experiments performed using the laboratory test-bed plotted in figures 8a, 9a and 10a (all in blue color) showed the dynamic and complex nature of the non-linear friction phenomena. The model parameters identified from the experiments through system identification listed in table 5 were substituted in the novel friction model structure and subsequently used to model friction features in the various regions of interest namely the constant velocity, pre-slide displacement and frictional-lag figures (8a, 9a and 10a) respectively. The results of these were plotted against the corresponding graphs obtained from the lab experiments as shown in the figures. The error measures (MSE), in tables 3 and 4, and the plots showed the model to closely replicate observed friction dynamics of the laboratory test-bed. For the pre-slide experiment of figure 9a, the result showed some quantization. This is due to the fact that the range of the torque sensor used in the experiment was larger than the torque exerted in the pre-slide regime. Model parameter estimation of the LuGre and GMS models was carried out and the results presented in tables 6 and 7 alongside that of the proposed model for the prediction of the pre-slide hysteresis and frictional lag respectively. From these tables the proposed friction model showed a greater prediction accuracy than the LuGre and GMS models.

Results of the validation experiments performed with the laboratory test-bed were plotted figures 8b, 9b and 10b representing respectively the gross slide, pre-slide and frictional lag regions. These experiments were performed using different input variables from those used for the friction characterization (identification) exercise. In the same token, the proposed model structure with identified parameters in table 5 was used to model friction behaviour in the various regimes. The result of the model validation showed the model parameters obtained to yield a parsimonious model able to capture known friction dynamics as reflected in figures 8b, 9b and 10b as well as the MSE in tables 3, 4, 6 and 7. These figures and tables indicate the Proposed friction model is able to model known features of friction obtained from the test-bed with low number of parameters (7) which are easy to estimate like the LuGre model with 6 parameters but not able to adequately capture true pre-slide friction hysteresis with non-local memory. The LuGre model also suffers from positional drift

in the pre-slide regime while the novel model presented exhibits non drift property of true friction. Though the GMS is able to capture accurately pre-slide hysteresis with non-local memory and exhibits non drift, it however requires a large number of parameters to capture these features. This makes its implementation and parameter estimation very difficult. This feature makes the proposed friction model novel.

The validation result suggests that proposed friction model is able to predict true friction better than the GMS and LuGre models.

### 7. CONCLUSION

A novel friction model structure capable of predicting known static and dynamic phenomena of friction has been presented in detail in this paper. Results of the various experiments carried out on a laboratory friction test-bed reflect the rich dynamics of the friction phenomena and shows agreement with most experimentally observed friction features. The proposed friction model being simple both in structure and implementation demonstrates superior capability for friction prediction in systems for control and simulation when compared with the LuGre and GMS models. Further research studies should focus on making the novel friction model adaptive and then subsequently implementing it for friction compensation.

### References

Al-Bender, F., Lampaert, V. and Swevers, J. (2004) 'Modeling of dry sliding friction dynamics: From heuristic models to physically motivated models and back', *Chaos: American Institute of Physics Inc.*, 14(2), pp. 446–460. doi: 10.1063/1.1741752.

Al-Bender, F., Lampaert, V. and Swevers, J. (2005) 'The generalized Maxwell-slip model: a novel model for friction Simulation and compensation', *IEEE Transactions on Automatic Control*, 50(11), pp. 1883–1887. doi: 10.1109/TAC.2005.858676.

Al-duwaish, H. N. (1999) 'Parameterization and Compensation of Friction Forces Using Genetic Algorithms', *Dynamical Systems*, 00(c), pp. 653–655. doi: 0-7803-5589-X/99/.

Altpeter, F. (1999) *Friction Modeling , Identification and Compensation*. Ecole Polytechnique Federale De Lausanne. doi: 10.5075/epfl-thesis-1988.

Armstrong-Helouvry, B., Dupont, P. and Wit, C. C. De (1994) 'A Survey of Models, Analysis Tools and Compensation Methods for the Control of Machines with Friction', *Automatica*, 30(7), pp. 1083–1138. doi: 0005-1098/94.

Bai, E.-W. (1997) 'Parametrization and adaptive compensation of friction forces.pdf', *International Journal of Adaptive Control and Signal Processing*, 11, pp. 21–31.

Canudas de Wit, C. *et al.* (1995) 'A new model for control of systems with friction', *IEEE Transactions on Automatic Control*, 40(3), pp. 419–425. doi: 10.1109/9.376053.

Dahl, P. R. (1968) 'A solid friction model', in *Technical Report TOR-01 58(3 107-1 8)- 1*. El Segundo, CA, 158. USA: Aerospace Corporation. doi: TOR-0158(3107-18)-1.

Desrayaud, G. *et al.* (2013) 'Revisiting the LuGre Model Stick-slip motion and rate dependence', *International Journal of Thermal Sciences, Elsevier*, 72, pp. 18–33.

Dhaouadi, R. and Ghorbel, F. (2008) 'Modelling and analysis of non-linear stiffness, hysteresis and friction in harmonic drives and gears', *International Journal of Modelling and Simulation*, 28(3), pp. 329–336. doi: 0232929032000115137.

Drincic, B. (2012) *Mechanical Models of Friction That Exhibit Hysteresis , Stick-Slip , and the Stribeck Effect*. The University of Michigan.

Dupont, P. *et al.* (2002) 'Single state elastoplastic friction models', *IEEE Transactions on Automatic Control*, 47(5), pp. 787–792. doi: 10.1109/TAC.2002.1000274.

Dupont, P., Armstrong, B. and Hayward, V. (2000) 'Elasto-plastic friction model: contact compliance and stiction', in *Proceedings of the 2000 American Control Conference. ACC (IEEE Cat. No.00CH36334)*. IEEE, pp. 1072–1077 vol.2. doi: 10.1109/ACC.2000.876665.

Dupont, P. E. and Dunlap, E. P. (1995) 'Friction Modeling and PD Compensation at Very Low Velocities', *Journal of Dynamic Systems, Measurement, and Control*, 117(1), pp. 8–14. doi: 10.1115/1.2798527.

Geffen, V. Van (2009) *A study of friction models and friction compensation*. Eindhoven. doi: 2009.118.

Grami, S. and Gharbia, Y. (2017) 'Identification of GMS friction model using a new switching function: Experimental investigation', *International Journal of Modelling, Identification and Control*, 27(1), pp. 31–39. doi: 10.1504/IJMIC.2017.082490.

Guenther, R. *et al.* (2006) 'Cascade controlled pneumatic positioning system with LuGre model based friction compensation', *Journal of the Brazilian Society of Mechanical Sciences and Engineering*, 28(1), pp. 48–57. doi: 10.1590/S1678-58782006000100006.

Haessig, D. A. and Friedland, B. (1991) 'On the Modeling and Simulation of Friction', *Journal of Dynamic Systems, Measurement, and Control*, 113(3), pp. 1256–1261. doi: 10.1115/1.2896418.

Hess, D. P. and Soom, A. (1990) 'Friction at a Lubricated Line Contact Operating at Oscillating Sliding Velocities', *Journal of Tribology*, 112(1), p. 147. doi: 10.1115/1.2920220.

Khayati, K., Bigras, P. and Dessaint, L.-A. (2009) 'LuGre model-based friction compensation and positioning control for a pneumatic actuator using multi-objective output-feedback control via LMI optimization', *Mechatronics*. Elsevier Ltd, 19(4), pp. 535–547. doi: 10.1016/j.mechatronics.2008.12.006.

Lampaert, V., Al-Bender, F. and Swevers, J. (2003) 'A generalized Maxwell-slip friction model appropriate for control purposes', in *IEEE International Workshop on Workload Characterization (IEEE Cat. No.03EX775)*. IEEE, pp. 1170–1177. doi: 10.1109/PHYCON.2003.1237071.

Lu, L. *et al.* (2009) 'Adaptive robust control of linear motors with dynamic friction compensation using modified LuGre model', *Automatica*. Elsevier Ltd, 45(12), pp. 2890–2896. doi: 10.1016/j.automatica.2009.09.007.

Nnaji, A. C. (2012) *Introduction to control systems*. Enugu, Nigeria: De-Sanctity Publications.

Nnaji, A. C. (2017) *Modelling and control of velocity and position drives subject to friction*. University of Reading, United Kingdom.

Olsson, H. (1996) *Control Systems with Friction. PhD thesis*. Lund Institute of Technology (LTH).

Rabinowicz, E. (1958) 'The Intrinsic Variables affecting the Stick-Slip Process', *Proceedings of the Physical Society*, 71(4), pp. 668–675. doi: 10.1088/0370-1328/71/4/316.

Reynolds, O. (2014) 'Theory of Lubrication and its Application to Mr . Beauchamp Tower's Experiments, Including an Experimental Determination of the Viscosity of Olive Oil', in *Philosophical transactions of The Royal Society of London*. The Royal Society, pp. 157–234. Available at: http://www.jstor.org/stable/109480 .

Saleem, A., Al Ratrout, S. and Wong, C. B. (2017) 'Nonlinear component-based modelling and hardware-in-the loop simulation of servo-pneumatic systems', *International Journal of Modelling, Identification and Control*, 28(1), pp. 40–57. doi: 10.1504/IJMIC.2017.085297.

Stribeck, R. (1902) 'Die wesentlichen eigenshaften der gleit-und rollenlager- The Key Qualities of sliding and roller bearings', *VDI-Zeitschrift Seutscher Ingenieure*, 46(38, 39), pp. 1341–1348, 1432–1438.

Swevers, J. *et al.* (2000) 'An integrated friction model structure with improved presliding behavior for accurate friction compensation', *IEEE Transactions on Automatic Control*, 45(4), pp. 675–686. doi: 10.1109/9.847103.

Vargas, F. J. T., De Fieri, E. R. and Castelan, E. B. (2004) 'Identification and friction compensation for an industrial robot using two degrees of freedom controllers', in *ICARCV 2004 8th Control, Automation, Robotics and Vision Conference, 2004*. IEEE, pp. 1146–1151. doi: 10.1109/ICARCV.2004.1469006.

Xiang, H., Qiu, Z. and Li, X. (2009) 'Simulation and experimental research of non-linear friction compensation for high-precision ball screw drive system', in *9th International Conference on Electronic Measurement & Instruments*. IEEE, pp. 3-604-3–609. doi: 10.1109/ICEMI.2009.5274257.

Xiong, X., Kikuuwe, R. and Yamamoto, M. (2012) 'A Differential-Algebraic Multistate Friction Model', in *Lecture Notes in Computer Science (including subseries Lecture Notes in Artificial Intelligence and Lecture Notes in Bioinformatics)*, pp. 77–88. doi: 10.1007/978-3-642-34327-8_10.

Xiong, X., Kikuuwe, R. and Yamamoto, M. (2013) 'A Multistate Friction Model Described by Continuous Differential Equations', *Tribology Letters*, 51(3), pp. 513–523. doi: 10.1007/s11249-013-0187-x.

Zhao, L. and Zhang, W. (2019) 'Survey and tutorial on multiple model methodologies in modelling, identification and control', *International Journal of Modelling, Identification and Control*, p. 1. doi: 10.1504/ijmic.2019.10023531.
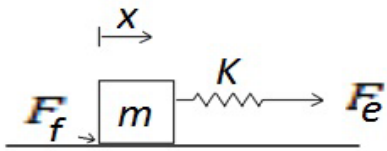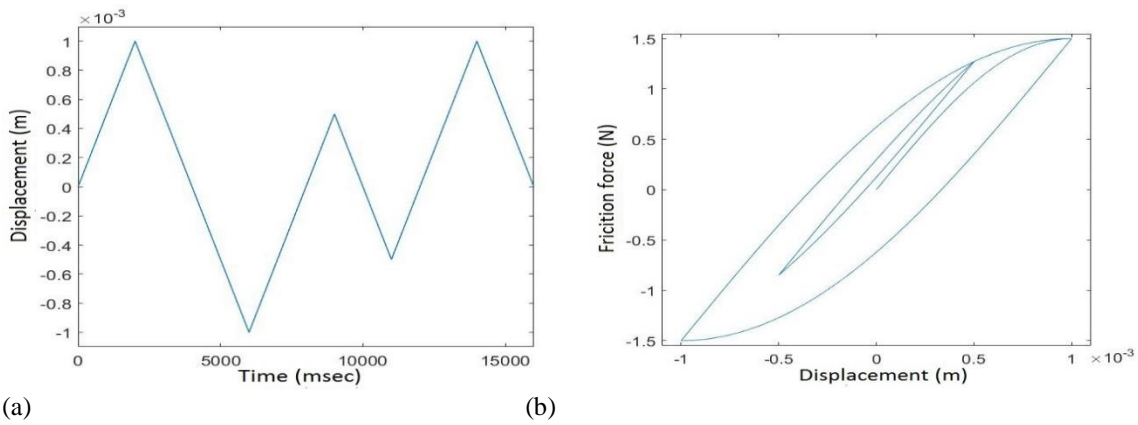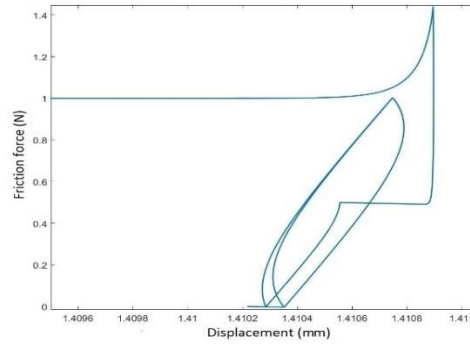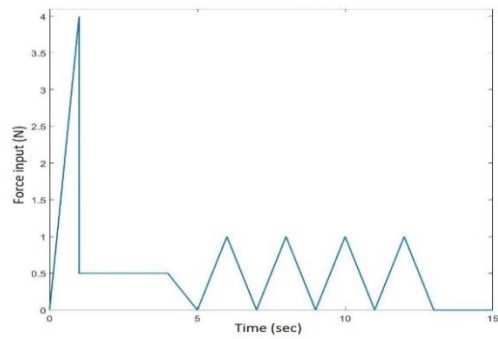
**Figures**



Fig. 1. A simple mass-spring system used for simulation purposes.



(a)                                                                                    (b)

Fig. 2. Simulation result for pre-sliding friction hysteresis with non-local memory features using the novel friction model; (a) Reference displacement input variable and (b) The friction displacement plot.

(a)                                                    (b)

Fig. 3. Simulation result for the non-drift friction feature using the novel friction model (a) The applied force and (b) Plot of the friction against displacement for the pre-slide friction regime
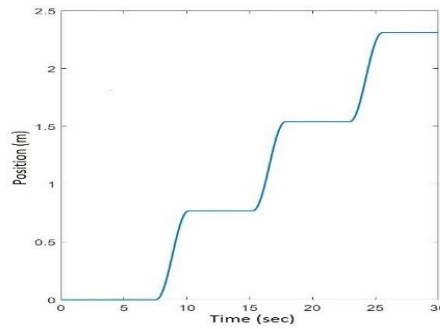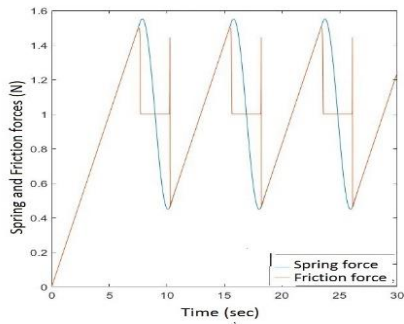


(a)                                                    (b)

Fig. 4. Simulation results for the stick-slip motion using the proposed friction model (a) The friction and spring forces against time and (b) The velocity plot against time showing periods of stick and slip motions.
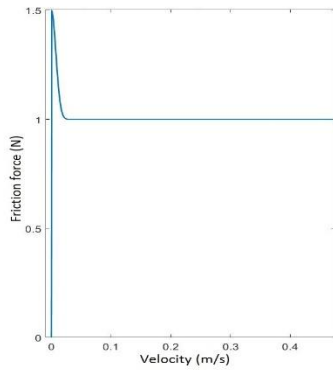


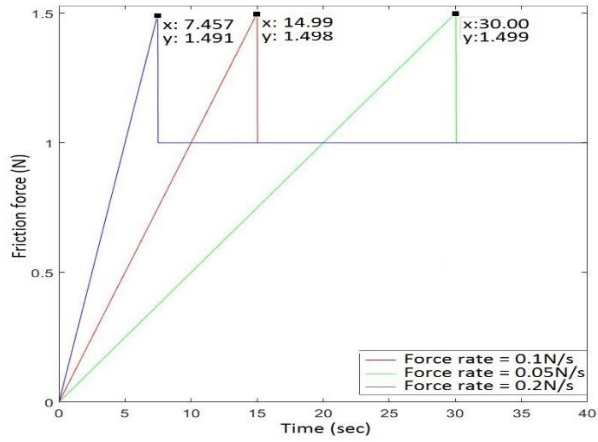Fig. 5. Simulation of the friction velocity relationship (Stribeck effect) using the novel friction model

Fig. 6. Varying breakaway friction force prediction with the novel friction Model
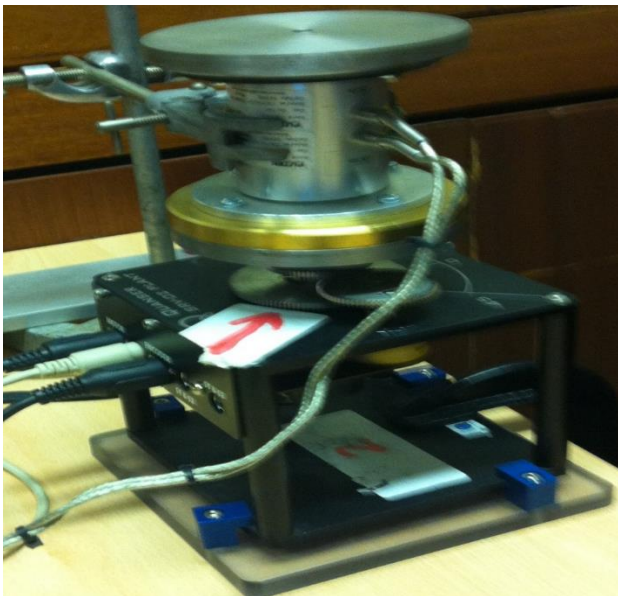


Fig. 7. Experimental test-bed set-up for friction characterization



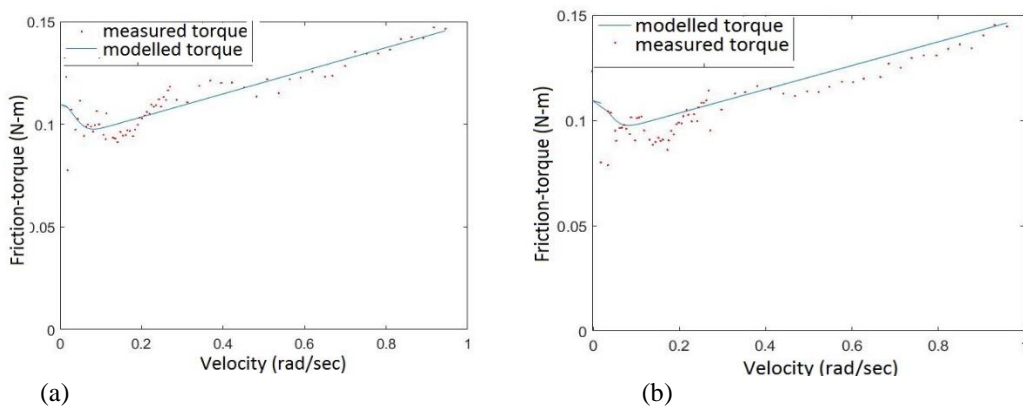(a)                                                                (b)

Fig. 8. Constant velocity friction characterization experiments showing; (a) Model parameter identification result, and (b) Model validation result and validation data.
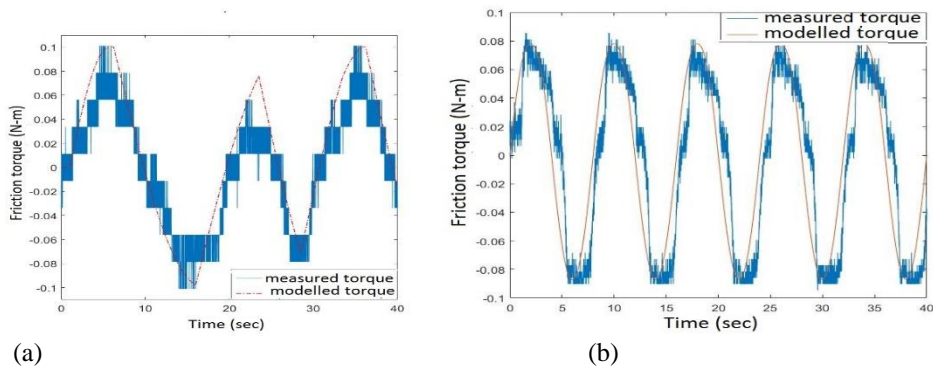
Fig. 9. Pre-sliding friction characterization experiment; (a) Model parameter identification result, and (b) Model validation result and validation data.
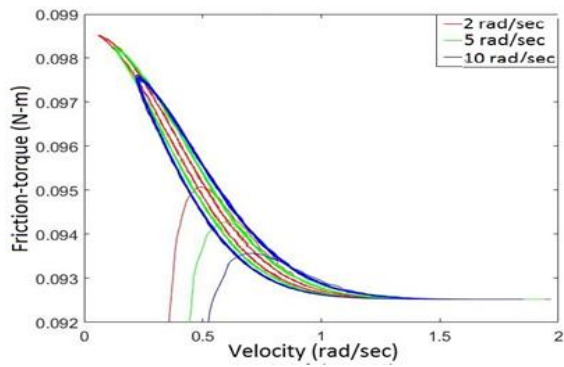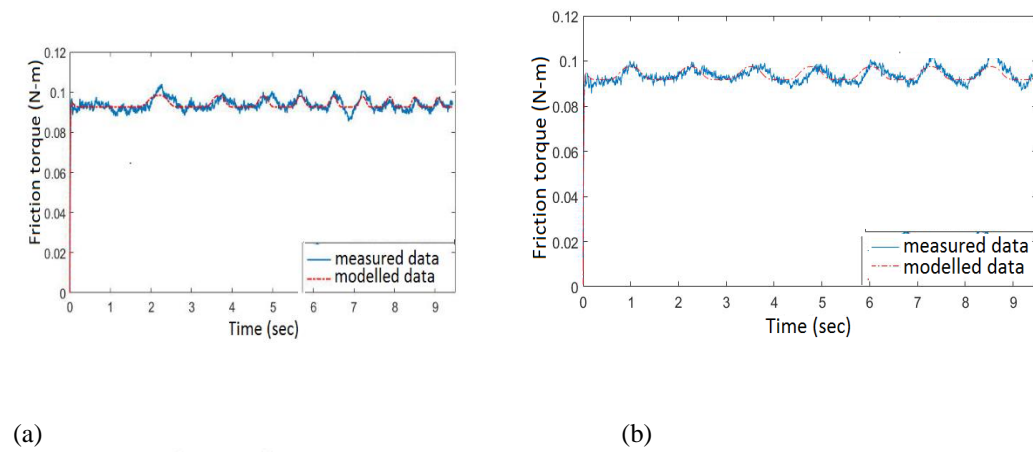






Fig. 10. Frictional-lag characterization experiment; (a) Model parameter identification result with identification data, (b) Model validation result and validation data, and (c) frictional lag feature of the novel friction model showing how acceleration and deceleration affect the Stribeck friction force for various velocities

**Tables**

Table 1: Key attributes of some dynamic friction models in terms of their ability to predict relevant friction features and ease of identification and implementation

| Model | Hysteresis | Non-drift | Stribeck | ID & Imp |
|-------|-----------|-----------|----------|----------|
| LuGre | No | No | Yes | Yes |
| E-P | No | Yes | Yes | Yes |
| GMS | Yes | Yes | Yes | No |
| Xiong | Yes | Yes | Yes | No |

Table 2: Parameter values of the novel friction model used for friction simulation.

| Parameter | Name and unit | Value |
|-----------|---------------|-------|
| $F_s$ | Static friction (N) | 1.5 |
| $F_c$ | Coulomb friction (N) | 1.0 |
| $v_s$ | Stribeck velocity (m/s) | 0.001 |
| $Z_b$ | Breakaway displacement (m) | 0.001 |
| $\sigma$ | Micro-damping (Ns/m) | $\sqrt{100000}$ |
| $\tau$ | Frictional lag (s) | 0.002 |

Table 3: Identified static parameters value for the novel friction model

| Model parameter | Estimated value | MSE ($10^{-5}$) |
|-----------------|-----------------|-----------------|
| $F_s$ | 0.0994 | |
| $F_c$ | 0.0929 | |
| $v_s$ | 0.1407 | |
| $f_v$ | 0.0603 | |
| Estimation error | | 3.7316 |
| Validation error | | 5.4988 |

Table 4: Estimated and Mean square error values for the dynamic parameters of the novel friction model.

| Model parameter | Value | MSE ($10^{-6}$) |
|-----------------|-------|-----------------|
| $\sigma$ | 0.0174 | |
| $Z_b$ | 0.0060 | |
| $\tau$ | 0.0130 | |
| Estimation error | | 4.4688 |
| Validation error | | 5.3081 |

Table 5: Estimated parameters value for the novel friction model

| Model parameter | Estimated value |
|-----------------|-----------------|
| $F_s$ | 0.0994 |
| $F_c$ | 0.0929 |
| $v_s$ | 0.1407 |
| $\sigma$ | 0.3213 |
| $Z_b$ | 0.0060 |
| $\tau$ | 0.0130 |
| $f_v$ | 0.0603 |

Table 6: Performance comparison of the various friction models for pre-slide friction prediction in terms of MSE for both estimation and validation

| Model | Estimation MSE ($10^{-5}$) | Validation MSE ($10^{-5}$) |
|---|---|---|
| Proposed | 8.3762 | 9.5132 |
| LuGre | 8.6065 | 10.091 |
| GMS | 8.6428 | 9.7653 |

Table 7: Performance comparison of the various friction models for gross-slide friction prediction in terms of MSE for both estimation and validation.

| Model | Estimation MSE ($10^{-4}$) | Validation MSE ($10^{-4}$) |
|---|---|---|
| Proposed | 3.6074 | 8.9796 |
| LuGre | 3.8059 | 9.6759 |
| GMS | 3.8059 | 9.7548 |